Potential-Modulated, Attenuated Total Reflectance Spectroscopy of Poly(3,4-ethylenedioxythiophene) and Poly(3,4-ethylenedioxythiophene Methanol) Copolymer Films on Indium−Tin Oxide

Walter J. Doherty III,‡ Ronald J. Wysocki, Jr., Neal R. Armstrong,* and S. Scott Saavedra*

Department of Chemistry, University of Arizona, Tucson, Arizona 85721

Received: October 28, 2005; In Final Form: January 4, 2006

We report the first application of a potential-modulated spectroelectrochemical ATR (PM-ATR) instrument utilizing multiple internal reflections at an optically transparent electrode to study the charge-transfer kinetics and electrochromic response of adsorbed films. A sinusoidally modulated potential waveform was applied to an indium−tin oxide (ITO) electrode while simultaneously monitoring the optical reflectivity of thin (2−6 equivalent monolayers) copolymer films of poly(3,4-ethylenedioxythiophene) (PEDOT) and poly(3,4-ethylenedioxythiophene methanol) (PEDTM), previously characterized in our laboratory.[1] At high modulation frequencies the measured response of the polymer film is selective toward the fastest electrochromic processes in the film, presumably those occurring within the first adsorbed monolayer. Quantitative determination of the electrochromic switching rate, derived from the frequency response of the attenuated reflectivity, shows a linear decrease in the rate, from 11×10^3 s^{-1} to 3×10^3 s^{-1}, with increasing proportions of PEDTM in the copolymer, suggesting that interactions between the methanol substituent on EDTM and the ITO surface slow the switching process by limiting the rate of conformational change in the polymer film.

Introduction

Thin films of poly(alkylenedioxythiophene) polymers undergo reversible electrochromic transitions, in which the visible absorption band of the neutral form shifts to the near-infrared upon oxidation, changing the film from darkly colored to nearly transparent.[2−13] These materials, especially poly(3,4-ethylenedioxythiophene) (PEDOT) and its derivatives (Figure 1), have been studied extensively to optimize their spectroscopic and electrochemical properties for use in display applications. Reynolds and co-workers[5−8,14] have demonstrated that the spectroelectrochemical properties of PEDOT derivatives can be largely controlled through modifications of the polymer backbone via the substituents added to the EDOT and through the formation of copolymers with these modified monomers. Several major effects have been observed to depend on the nature of the substituent group, such as the potential required for polymerization and oxidation[13,15,16] and the optical properties of the polymer, including the optical band gap and the degree of electrochromic contrast during changes in the redox state.[5,8,9,17]

These previous studies have also demonstrated that the use of monomers with large substituents, or increasing the size of the alkylenedioxy bridge, significantly affect the rate at which the optical properties of the polymerized film can be "switched", or cycled, between the reduced and oxidized forms.[5−7] In most experiments a potential step is applied to the electrode, and the time required to achieve a certain percentage of the full transmittance contrast is measured. Switching times, to 95% of the full transmittance contrast, have ranged from 2 s to <1 s for thin films of PEDOT and C_{14}-alkyl- or phenyl-modified PEDOT, respectively.[7] These differences are attributed to differences in film density. Polymers with larger substituent groups form a less dense film, allowing rapid diffusion of counterions, and therefore exhibit relatively faster electrochromic switching rates.

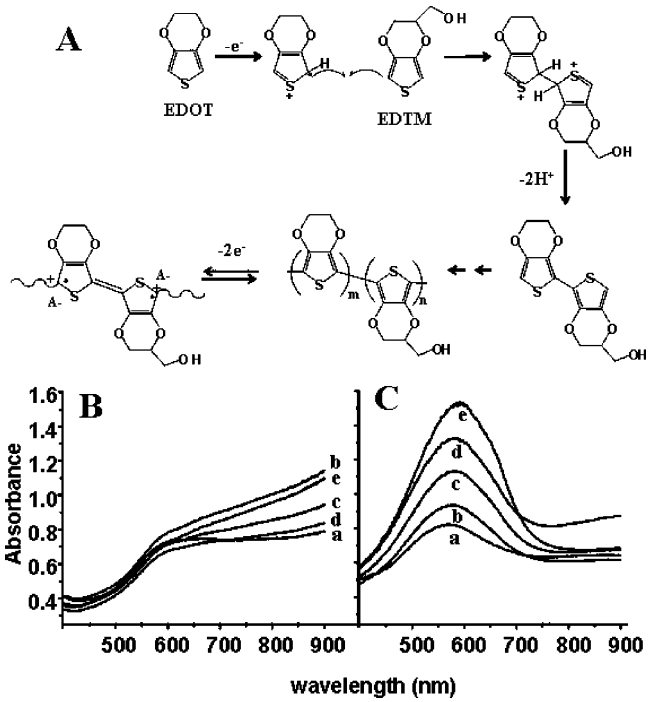

Figure 1. (A) The copolymerization scheme for EDOT and EDTM. The electrochromic behavior of PEDOT and PEDTM is observed in the absorbance spectra of homo- and copolymer films in the oxidized (B) and reduced (C) state. The molar absorptivity of the reduced film increases substantially with increasing mole fraction of EDTM in the comonomer solution: 0% (a), 25% (b), 50% (c), 75% (d), and 100% EDTM (e). See ref 1.

* To whom correspondence should be addressed. Phone: (520) 621-8242 (NRA); (520) 621-9761 (SSS). Fax: (520) 621-8407.

‡ Current address: Department of Physics and Measurement Technology (IFM), Linköping University, SE-581 83 Linköping, Sweden.

10.1021/jp056230n CCC: $33.50
Published on Web 02/18/2006

Our recent studies have focused on the use of PEDOT "wires" to connect ferrocene-modified and EDOT-modified PAMAM dendrimers in porous sol−gel films on ITO substrates[18] and copolymer thin films of PEDOT and poly(3,4-ethylenedioxythiophene methanol) (PEDTM).[1] In both cases the presence of the EDTM monomer in the PEDOT chain appears to influence both the oxidation/polymerization potentials and the optical band gap of the resultant polymer. Figure 1 shows significant changes in the molar absorptivity of the polymer as a function of oxidation state and the degree of substitution (through copolymerization with EDTM) along the polymer backbone.[1] Understanding electron-transfer events in ultrathin films of conducting polymers is important, as such events control the photoelectrochemical activity of nanoparticles attached to a PEDOT chain or the electrochemical reactivity of copolymers of PEDOT with monomers which provide for its robust attachment to an ITO surface.[19−22]

Electroreflectance (ER) spectroscopy is ideally suited for temporal studies of electrochromic effects and spectroelectrochemical behavior in such polymeric ultrathin films on electrode surfaces. In ER spectroscopy, the intensity of light reflected by the electrode surface is monitored while an ac potential modulation is applied simultaneously to the electrode, as represented by the following expressions

$$E = E_{dc} + E_{ac} \sin \omega t \tag{1a}$$

$$\mathscr{R} = \mathscr{R}_{dc} + \mathscr{R}_{ac} \sin(\omega t - \theta) \tag{1b}$$

where E represents the overall potential applied to the electrode, E_{dc} is the time-average potential, and E_{ac} is the amplitude of the potential modulation. Analogously, $\mathscr{R}$ represents the overall reflectance of the probe beam, $\mathscr{R}_{dc}$ is the time-average reflectance, $\mathscr{R}_{ac}$ is the amplitude of the modulated reflectance induced by E_{ac}, ω is the modulation frequency, θ is the phase angle between E_{ac} and $\mathscr{R}_{ac}$, and t is time. Changes in the reflectivity represent changes in the optical constants of the film[19−21] caused by one or more physical changes, such as changes in oxidation state, local charge density, and molecular conformation. The frequency response of the reflectance can provide information about apparent rates of electron transfer, especially for those redox events which induce changes in electrochromic properties at the electrode/polymer interface. From a molecular perspective, determination of effective switching times can provide valuable insight into the kinetic parameters and rate-limiting mechanisms behind the redox-driven changes in optical properties of ultrathin polymer films.

Theoretical aspects of ER spectroscopy and ER spectroelectrochemical techniques have been developed by Niki and Sagara,[23−25] and have been used extensively to investigate electron transfer processes and rates for molecular adlayers at reflective electrode surfaces. Studies reported to date have primarily used external reflection and surface plasmon resonance geometries to monitor changes in film optical properties. For example, the adsorption and electron transfer kinetics of relatively small molecular adsorbates such as hemin,[24,26−28] methylene blue,[29,30] and Nile Blue[24,25] have been studied on highly oriented pyrolytic graphite (HOPG). Gold modified with monolayers of alkanethiols is another common electrode surface for ER spectroscopy and has been used to study covalently bound ruthenium complexes,[31] porphyrins.,[32,33] nanoparticle films,[34−36] and adsorbed protein films composed of azurin,[37] putaredoxin, [38] and cytochrome *c*.[23,34,39−43]

ER spectroscopy has also been performed in a transmission geometry, using an optically transparent electrode. Fujishima and co-workers[44−47] utilized this adaptation to differentiate kinetically heterogeneous processes in polypyrrole films on tin oxide (SnO_2). This approach has also been used to study electron injection into CdS and Au nanoparticles from SnO_2[34] and modified indium−tin oxide (ITO),[36] respectively, and to characterize the electrochromic switching of ruthenium dioxylene complexes adsorbed to porous, nanocrystalline SnO_2.[48] In the latter study, it was determined that the rate of optical switching was limited by the RC time constant of the electrochemical cell, rather than electron-transfer kinetics.[48] Work by Scherson et al.[49] emphasizes another possible limitation of ER spectroscopy due to film anisotropy or changes in the optical properties of the electrode surface itself as a function of applied potential (*intrinsic electroreflectance*).

The sensitivity of transmission and external reflection ER geometries may be inadequate when the sample is a thin, weakly absorbing molecular film. Higher sensitivity for thin film applications may be obtained by using an attenuated total reflection (ATR) geometry, wherein the probe beam is internally reflected multiple times down the length of a transparent planar waveguide electrode (e.g., an ITO-coated, glass microscope slide).[50] This work describes the first reported implementation of multiple internal reflection ATR spectroscopy operating under potential modulation (PM-ATR), and its application to study electrooptical transition kinetics in thin adlayer films. Thin polymer and copolymer films (2−6 monolayers) of PEDOT and PEDTM[1] (Figure 1) are used as an exemplary system to illustrate the effectiveness of this technique. We also show the use of the theoretical framework developed by Niki and Sagara[23−25] to extract an apparent heterogeneous charge-transfer rate, or rate of spectroelectrochemical switching, as a function of copolymer composition.

Experimental Section

Unless otherwise stated, all chemicals were supplied by Aldrich and used without further purification. 3,4-Ethylenedioxythiophene methanol (EDTM) was synthesized in the Organic Synthesis Facility at the University of Arizona according to procedures outlined by Lima[51] and Akoudad.[52] Solutions of both EDOT and EDTM were prepared by dissolving the monomer in methanol and then diluting this solution 10-fold (v/v) with an aqueous solution of 0.11 M $LiClO_4$ to a final monomer concentration of 10 mM.

Electrochemical cell parameters, solution resistance (R_s) and double-layer capacitance (C_{dl}), were determined by electrochemical impedance spectroscopy and scan rate dependent voltammetry.[53] All electrochemical measurements were performed on an EG&G Princeton Applied Research Model 263A potentiostat/galvanostat. Impedance measurements were obtained with an EG&G Princeton Applied Research Model 5209 Lock-In amplifier operated with PowerSuite 2.00.5 software.

Figure 2 is a schematic diagram of the PM-ATR experimental setup. The electrochemical ATR apparatus has been described elsewhere.[50,54] Briefly, a collimated (diameter ∼1 mm) beam of white light (WL in Figure 2) is coupled into an ITO-coated glass substrate (ca. 1 mm thickness). The ITO thin film is the working electrode in a three-electrode cell, consisting of a Ag/AgCl reference electrode (Bioanalytical Systems) and a Pt wire counter electrode, interfaced to the potentiostat (PS). The ITO surface dimensions were 71 mm × 2 mm, with the ATR beam propagating along the long axis, at an internal reflection angle (β) of 63° to 64° relative to the surface normal. Incoupling prisms were positioned 40 mm apart, producing approximately 10 reflections at the ITO/electrolyte interface.

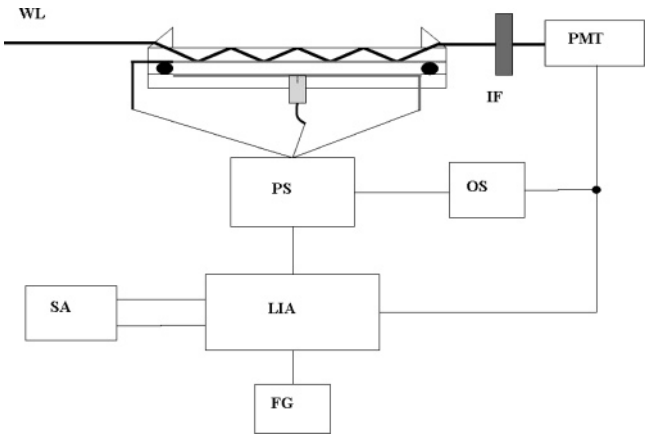

Figure 2. The experimental setup for PM-ATR spectroscopy. White light (WL) is coupled into, and internally reflected down the length of, an ITO-coated glass microscope slide. The steady-state potential (E_{dc}) is set at the potentiostat (PS). The potential at the ITO electrode is modulated by applying a sinusoidal reference voltage from a lock-in amplifier (LIA) to the external input of the PS. The frequency of the modulation is set at the function generator (FG), which supplies a 5 V_{p-p} TTL external reference signal to the LIA. The optical signal, i.e., the transmitted intensity of the internally reflected beam, is monitored at 580 nm with a 20 nm band-pass interference filter (IF) and photomultiplier tube (PMT). Both the reference voltage and PMT output are monitored with an oscilloscope (OS). The PMT output is coupled to the LIA input and both the in-phase (Re($\mathscr{R}_{ac}$)) and 90° out-of-phase (Im($\mathscr{R}_{ac}$))components are recorded with a LabView signal averaging (SA) program.

This number of reflections represents a compromise between the enhanced sensitivity provided by a multiple reflection ATR geometry and the intrinsic ER response of ITO. It is well-known that the optical properties of ITO change as a function of applied potential as a result of changes in the free-electron population in the near-surface region.[55] If the optical path length in the ITO layer is small enough, this effect is negligible. Ten reflections provided adequate sensitivity to measure the ER response of the adlayer films examined here, but were insufficient for the ITO to make a significant contribution to the intrinsic ER response.

To ensure homogeneous current density across the electrode area, the Pt wire counter electrode was arranged parallel to the ITO surface, such that all areas of the ITO were approximately equidistant from the Pt wire. Polymer and copolymer films were electrodeposited onto the ITO surface by stepping the potential to 1.15 V and holding for 1 s. During this time approximately 1 to 3 mC/cm^2 of charge was passed, corresponding to deposition of 2−6 equivalent monolayers, assuming 10 Å^2 per monomer unit and 2.3 electrons transferred per monomer during deposition.[56]

To drive the potential modulation at the ITO electrode, a function generator (FG) (Krohn-Hite Model 5200) was used to supply a 5 V peak-to-peak square wave external reference to the lock-in amplifier (LIA) (Stanford Research Systems Model SR830). The amplitude of the reference output of the LIA was adjusted to the desired modulation amplitude and coupled to the external input of the potentiostat. The overall cell potential (E_{dc}) was controlled by using the potentiostat. This arrangement provides a sinusoidally modulated voltage (E_{ac}) applied to the ITO electrode about E_{dc}, which also serves as the reference signal for lock-in detection of the optical response. Unless otherwise stated, E_{ac} was set to 50 mV RMS (0.071 V peak-to-peak). The frequency of E_{ac} was set at the function generator and monitored on the LIA, with an analog oscilloscope (OS).

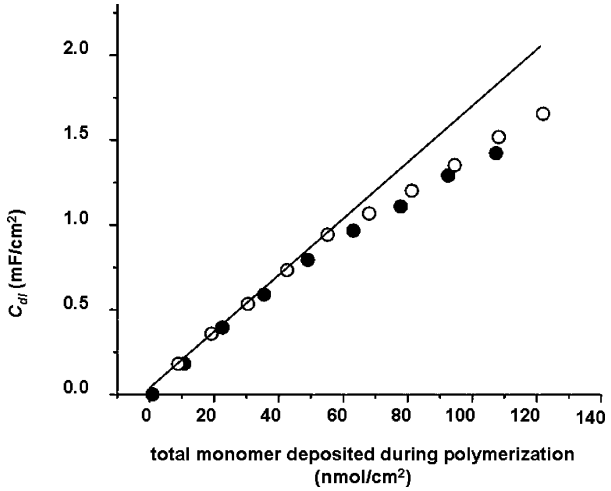

Figure 3. Double layer capacitance (C_{dl}) as a function of the amount of charge passed during electropolymerization of EDOT (●) and EDTM (○). The line represents the linear regression analysis of the data up to 60 nmol of monomer deposited per cm^2.

To monitor the optical response, the outcoupled beam was filtered with a 580 nm band-pass interference filter (IF) (fwhm 20 nm), then directed onto a photomultiplier tube (PMT), the output of which was monitored on the OS and fed into the input channel of the LIA. A LabView program was written to average the signal intensities of the in-phase (X) and 90° out-of-phase (Y) components over 15 s integration periods (SA).

Results and Discussion

Determination of Electrochemical Parameters. To model the frequency response of the ITO/PEDOT-PEDTM/solution interface, an equivalent circuit diagram was assumed based on those presented in refs 45 and 57−58 for adsorbed films of poly(pyrrole) and Prussian blue on ITO, respectively. In the absence of adsorbate-related charge-transfer processes, the electrochemical impedance response of the bare ITO surface can be represented by a simple series RC circuit consisting of the solution resistance (R_s), which includes the inherent resistance to charge flow through the ITO film, and the double-layer capacitance (C_{dl}).[45,57,58] Assuming this configuration, the impedance at high frequency becomes constant and limited to R_s. For the PM-ATR cell described above, R_s was found to be 34 ± 6 Ω·cm^2 by impedance spectroscopy. C_{dl} for the bare ITO electrode, measured by both impedance spectroscopy and scan rate dependent voltammetry, was 13 ± 4 μF/cm^2, resulting in a cell time constant (R_sC_{dl}) of 0.4 ± 0.1 ms.

The presence of a redox-active adlayer on the surface of the electrode necessitates adding components to the equivalent circuit. Faradaic electron-transfer processes between the adlayer and the electrode require additional capacitance (C_a) and charge-transfer resistance (R_{ct}) terms to adequately simulate the overall electrochemical response of the ensemble.[57,58]

As expected, electropolymerization and deposition of EDOT and/or EDTM onto the ITO surface had negligible effects on R_s. The uncertainty of ±6 Ω·cm^2 stated above is the standard deviation of values obtained on both bare and polymer-coated ITO substrates. In contrast, C_{dl} substantially increased after PEDOT/PEDTM film deposition and was proportional, at lower coverages of polymer, to the amount of charge passed during electropolymerization and the amount of polymer deposited. Figure 3 shows a linear ($R^2 = 0.997$) increase in C_{dl} for up to 60 nmol monomer deposited per cm^2, or approximately 30 equivalent monolayers. The capacitance begins to deviate from

linearity above 60 nmol/cm^2, presumably due to hindered counterion penetration or decreasing film conductivity.[51] Nearly identical behavior was observed for films composed of either PEDOT or PEDTM. An overall increase in double-layer capacitance per charge passed during polymerization was observed, represented by the slope of the linear component in Figure 3, corresponding to 18 ± 1 μF/nmol monomer deposited.

A similar linear increase in capacitance with charge passed during polymerization was obtained by Bobacka et al.[59] for the electropolymerization of PEDOT onto platinum from aqueous solutions. PEDOT deposition was observed to increase the total double-layer capacitance of the system by approximately 60 μF/nmol monomer deposited. This value was found to be independent of the concentration of supporting electrolyte, indicating that the capacitance is dominated by the number of electronic charge carriers within the polymer itself, i.e., polarons and bipolarons. The identical capacitative behavior obtained here for both PEDOT and PEDTM, shown in Figure 3, indicates that the number of charge carriers in both polymeric systems is nearly the same.

Potential-Modulated ATR. Upon oxidation, PEDOT/PEDTM polymers undergo a quasireversible spectroelectrochemical transition in which the absorbance maximum shifts from the visible to the near-IR (Figure 1). At the wavelength of maximum absorption ($\lambda_{max} = 571$ and 591 nm for PEDOT and PEDTM, respectively[1]) the neutral, reduced film has a molar absorptivity that is 1.2 and 2.2 times that of the oxidized film for PEDOT and PEDTM, respectively.[1] This change occurs over a very broad potential window between -0.5 and 0.5 V for PEDOT, and between -0.3 and 0.5 V for PEDTM. When E_{dc} is positioned within this potential window, E_{ac} induces changes in the molar absorptivity of the polymer film that are associated with changes in oxidation state.

If E_{ac} is positioned about the midpoint potential (E_{mid}, see Figure 5) for the redox couple, the relative amounts of the reduced and oxidized forms of the adlayer material are defined by the modified Butler−Volmer expression[23,25]

$$\frac{d(\Gamma_{red}/\Gamma_t)}{dt} = k_s\left[\left(1 - \frac{\Gamma_{red}}{\Gamma_t}\right)e^{(-\alpha nF/RT)(E-E_{mid})} - \frac{\Gamma_{red}}{\Gamma_t}e^{[(1-\alpha)nF/RT](E-E_{mid})}\right] \quad (2)$$

where k_s is the rate coefficient for heterogeneous electron transfer and α is the transfer coefficient. Γ_t and Γ_{red} represent the total surface coverage (moles/cm^2) of the adlayer and the coverage of the adlayer in the reduced form, respectively, and the other variables correspond to their accepted definitions. For optimal ER response, E_{dc} is set to the midpoint potential (E_{mid}) of the redox couple being investigated. We assume that E_{mid} represents a potential where ca. 50% of the conducting polymer is in its one-electron oxidized (polaron) state. $E - E_{mid}$ is therefore an "overpotential" applied to the electrode and represents the amplitude of E_{ac} at a given time. In the ATR configuration shown in Figure 2, the probe beam attenuation at each reflection is modulated by the change in molar absorptivity of the polymer induced by the application of a sinusoidally modulated E_{ac}. Figure 4 (inset) shows a schematic representation of the probe beam intensity that would be obtained while simultaneously modulating the potential on the ITO electrode. The modulation potential (E_{ac}) is superimposed on the overall potential applied to the electrode (E_{dc}). The corresponding ER response at λ_{max} is an oscillating probe beam intensity consisting of an AC component of the beam reflectivity ($\mathscr{R}_{ac}$) superimposed on the total steady-state reflectivity ($\mathscr{R}_{dc}$).

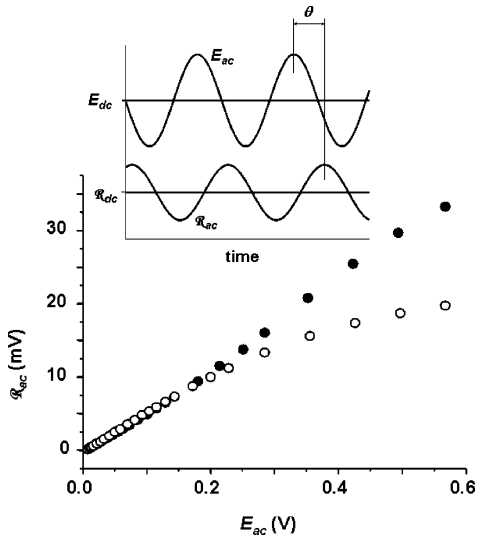

Figure 4. The ER response ($\mathscr{R}_{ac}$) at $E_{dc} = E_{mid}$ as a function of the potential modulation amplitude (E_{ac}) is shown for PEDOT (closed circles) and PEDTM (open circles) on ITO. The inset shows a schematic illustration of the modulation waveform (E_{ac}) centered about the steady-state potential E_{dc} that is applied to the ITO electrode. The resulting electroreflectance waveform ($\mathscr{R}_{ac}$) is superimposed on the steady-state ATR reflectance, $\mathscr{R}_{dc}$. The angle θ denotes the phase shift between E_{ac} and $\mathscr{R}_{ac}$. The relative magnitudes of E_{ac} and $\mathscr{R}_{ac}$ are arbitrarily assigned for illustration purposes.

Measuring the ER response as a function of the frequency of E_{ac} provides a means of determining the values of the Faradaic components of the equivalent circuit, R_{ct} and C_a.[24] Laviron has shown how the electrode rate constant, k_s, for a surface-confined redox couple, can be extracted from experimental values of R_{ct} and C_a by[60,61]

$$R_{ct} = \frac{2RT}{nn_aF^2k_s\Gamma_t} \quad (3a)$$

$$C_a = \frac{nn_aF^2\Gamma_t}{4RT} \quad (3b)$$

where nn_a is the product of the nominal and apparent number of electrons involved in the electrode reaction. Given these expressions, the electrode rate constant can be determined without regard for nn_a by

$$k_s = \frac{1}{2R_{ct}C_a} \quad (4)$$

The derivation of eqs 3a and 3b, however, assumes that the overpotential is small enough that a linear relationship is maintained between the Faradaic current and $E - E_{mid}$. This assumption is usually valid within a narrow potential window about E_{mid}. By analogy, to utilize eqs 3a and 3b, the amplitude of E_{ac} must be within this narrow potential range and a linear relationship obtained between E_{ac} and $\mathscr{R}_{ac}$. Niki et al. have shown, both experimentally and through simulation, that this assumption is generally applicable when $E_{ac} \ll RT/nF$.[25] In situations when $\mathscr{R}_{ac}$ is not proportional to E_{ac}, the use of eq 4 yields an overestimation of the apparent k_s.[23] Under circumstances in which a relatively large amplitude E_{ac} is necessary to generate an acceptable signal-to-noise, the nonlinearity of the ER response can be accounted for by solving eq 2 numerically.[23,31]

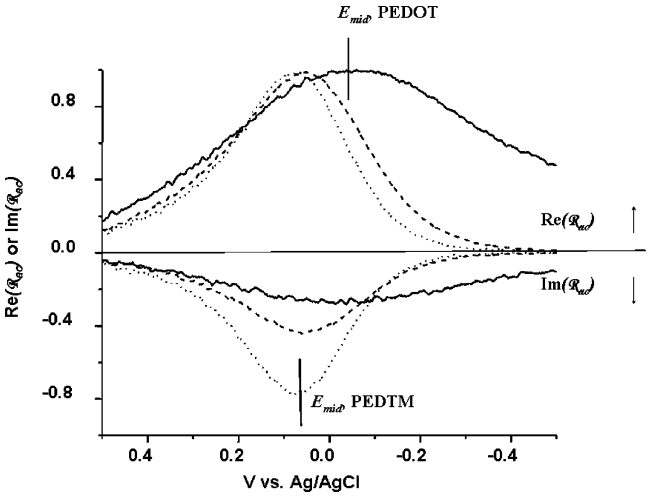

Figure 5. PM-ATR spectroelectrochemical anodic sweep voltammogram of thin films (2−6 monolayers) of PEDOT (—), PEDTM (···), and copolymer with 1:1 comonomer composition (- - -), obtained at a scan rate of 5 mV/s with modulation frequency and amplitude of 10 Hz and 50 mV rms, respectively. Both the real (Re($\mathscr{R}_{ac}$)) and imaginary (Im($\mathscr{R}_{ac}$)) components of the reflectance are shown. Data were normalized to unity at the maximum value of Re($\mathscr{R}_{ac}$).

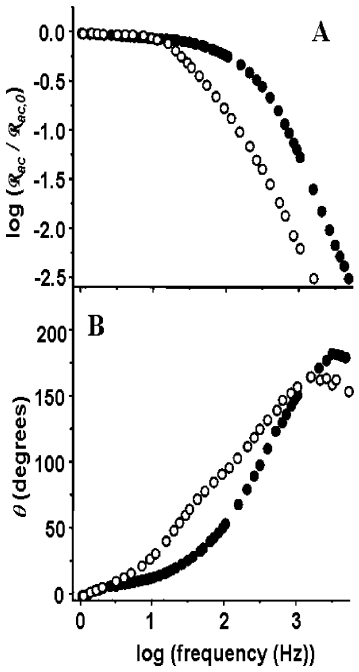

Figure 6. Electroreflectance response of PEDOT (●) and PEDTM (○). A Bode plot representing the magnitude of the AC component of the electroreflectance, $\mathscr{R}_{ac}$, as a function of frequency is shown in part A. The frequency dependence of the phase angle θ between E_{ac} and $\mathscr{R}_{ac}$ is shown in part B.

To determine the extent of linearity in the ER response of PEDOT/PEDTM films, E_{dc} was set at E_{mid} for PEDOT and PEDTM, determined by ER-detected voltammetry (Figure 5, discussed below). The magnitude of $\mathscr{R}_{ac}$ was measured as a function of the amplitude of E_{ac} at a modulation frequency of 10 Hz for approximately 10 equivalent monolayers of deposited monomer. Figure 4 shows the response for homopolymer films of PEDOT and PEDTM. PEDOT exhibited a wide linear range, extending to modulation amplitudes greater than 0.6 V. The PEDTM film maintained linearity up to approximately $E_{ac} = 0.2$ V, where the response began to plateau. The high degree of linearity observed for modulation amplitudes up to 0.15 V is demonstrated by the correlation coefficients (R^2 values) of 0.9996 and 0.9997 respectively obtained for pure PEDOT and PEDTM films. Thus the linear approximation used to derive the expressions in eqs 3 and 4 is valid at the 50 mV RMS (0.071 V) modulation amplitude used to drive the ER response of the PEDOT/PEDTM copolymer films. The intrinsic electroreflectance of bare ITO at 580 nm was found to be negligible over the range of potentials and modulation amplitudes applied.

The optimal E_{dc}, at which the maximum ER response is observed, was located by superimposing a linear sweep voltammogram on E_{ac} while monitoring the magnitude of $\mathscr{R}_{ac}$ at a modulation frequency of 10 Hz. Figure 5 shows the real and imaginary components of $\mathscr{R}_{ac}$ obtained during the anodic scan of the ER voltammograms. The peak shapes in the cathodic portion (not shown for clarity) were identical with those in the anodic portion, but were slightly shifted toward negative potentials. For PEDOT and PEDTM, the maximum ER response, $\mathscr{R}_{ac,max}$, is located at approximately −0.05 and 0.07 V, respectively, versus Ag/AgCl. For a copolymer film consisting of approximately equal proportions of both monomers,[1] the maximum ER response occurred at 0.05 V. The location of $\mathscr{R}_{ac,max}$ corresponds approximately to $E°$ values obtained by conventional voltammetry (0.08 V for PEDOT and 0.05 V for PEDTM).[1] The slight differences are likely due to the difficulty in assigning precise peak locations in the presence of the large non-Faradaic background inherent to conventional cyclic voltammetric measurements.

The peak width in Figure 5 represents the breadth of the potential window for electrochromic switching. The peak width for PEDOT films is much broader than that of both PEDTM and the 1:1 copolymer, indicating a wider distribution of redox states in the PEDOT film. This same response was noted by Akoudad and Roncali,[52] who observed narrow voltammetric peak widths for PEDTM relative to PEDOT. The ER voltammogram of the copolymer film indicates that the presence of EDTM disproportionately affects the electrochromic properties of the polymer. For a copolymer containing approximately equal proportions of both monomers, the peak location and width are similar to those of PEDTM.

The apparent electrode reaction rate, k_s, for a surface confined redox species can be assessed by simultaneously monitoring both the demodulation of $\mathscr{R}_{ac}$ relative to E_{ac} and the phase shift between E_{ac} and $\mathscr{R}_{ac}$ (see Figure 4 (inset)). Figure 6 shows the frequency dependence of $\mathscr{R}_{ac}$ and θ for films of PEDOT and PEDTM. To compare the films, the data sets were normalized to $\mathscr{R}_{ac} = 1$ and $\theta = 0$ at frequencies <1 Hz. The plot in Figure 6A shows that both polymers display similar frequency dependencies of reflectance with a plateau region at low frequencies and a sharp, monotonic drop in response at higher frequencies. The PEDOT response begins to deviate from the behavior seen at low frequencies above approximately 100 Hz, versus 20 Hz for PEDTM. Qualitatively, this indicates a faster overall rate of electrochromic switching, and a correspondingly more rapid apparent electrode reaction rate, for PEDOT relative to PEDTM. At 20 Hz, the PEDOT film is able to maintain approximately 90% of the initial magnitude of $\mathscr{R}_{ac}$, while $\mathscr{R}_{ac}$ for the PEDTM film has declined to approximately 65%. This suggests that charge transfer and ion motion in the thin polymer film are faster for PEDOT versus PEDTM.

Figure 6B shows the frequency dependence of θ for PEDTM and PEDOT films. The curves are roughly sigmoidal, with low- and high-frequency asymptotes. As observed for $\mathscr{R}_{ac}$, the curves begin to deviate from the low-frequency asymptote at ap-

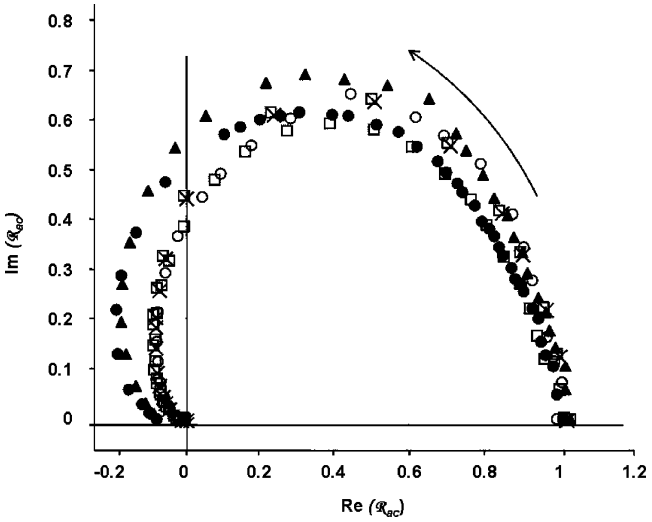

Figure 7. Complex plane plot of the electroreflectance response of PEDOT (●), PEDTM (○), and copolymers with EDOT mole fractions of 0.25 (□), 0.32 (×), and 0.53 (▲). The arrow indicates the direction of increasing frequency. The vertical line at Re($\mathscr{R}_{ac}$) = 0 represents the point at which the angular frequency (ω) is equal to $(2k_s/R_sC_{dl})^{1/2}$.

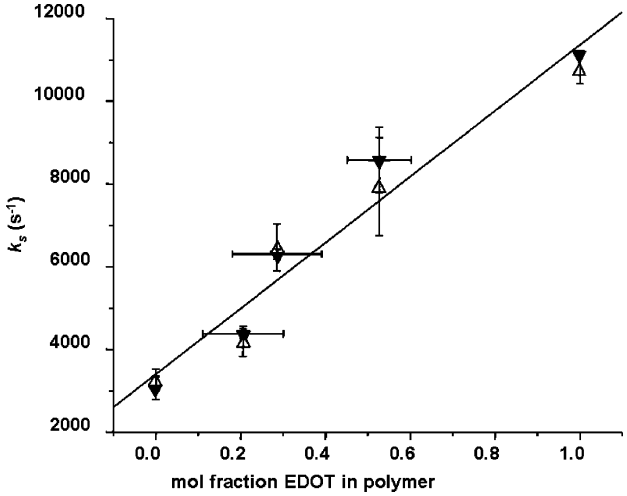

Figure 8. Electrooptical switching rate as a function of degree of copolymerization. Rate constants were obtained independently with either eq 6 and the complex plane plot (Figure 7) at Re($\mathscr{R}_{ac}$) = 0 (▼) or from eq 5 and the corresponding plot of ω cotθ vs $-\omega^2$ (△). The vertical error bars represent the standard deviation of multiple ER determinations of k_s. The horizontal error bars represent the uncertainty in the degree of copolymerization, due to measurements of the reactivity ratios given in ref 1. The solid line was obtained from linear regression analysis (R^2 = 0.962) of the average k_s values.

proximately 20 and 3 Hz for PEDOT and PEDTM, respectively. For PEDOT, θ increases to an inflection point at approximately 250 Hz and reaches a high-frequency limit at 180°. The curve increases smoothly, suggesting that the process responsible for the ER response can be described by a single apparent rate, or a continuous distribution of rates. For PEDTM, the phase angle increases to an inflection point at approximately 75 Hz, reaching a high-frequency limit at 165°. In contrast to the PEDOT curve, the PEDTM curve contains a slight shoulder near 50 Hz, indicating a significant difference in the dominant rate constant at low and high frequencies. This may be indicative of interactions between the hydroxyl group of PEDTM and the ITO surface inducing differentiation of adsorption sites on ITO, or causing differences in the switching rates between the first and subsequent adsorbed monolayers. For both films, the low signal-to-noise at high frequencies causes a slight decline in θ above 3 kHz.

A convenient graphical method to extract the apparent electrode rate constant is to construct a complex plane plot in which the imaginary, or 90° out-of-phase, component of $\mathscr{R}_{ac}$ (Im($\mathscr{R}_{ac}$)) is plotted against the real, or in-phase, component of $\mathscr{R}_{ac}$ (Re($\mathscr{R}_{ac}$)) (analogous to a Cole−Cole plot in electrochemical impedance spectroscopy).[24] Data for PEDOT and PEDTM homopolymers and several copolymer compositions are plotted in Figure 7 in this format using normalized values of $\mathscr{R}_{ac}$ and θ, as above, to calculate Re($\mathscr{R}_{ac}$) and Im($\mathscr{R}_{ac}$). Each polymer film produces a hemispherical plot. At low frequencies, θ is small and the in-phase component, Re($\mathscr{R}_{ac}$) is unity. In the high-frequency limit, both components are minimized as the overall value of $\mathscr{R}_{ac}$ approaches zero.

Niki et al.[24] have derived expressions that describe the frequency dependence of $\mathscr{R}_{ac}$ and θ in terms of the equivalent circuit components,[45,57,58] allowing the Faradaic time constant, $R_{ct}C_a$, to be determined graphically according to

$$-\omega \cot\theta = -\omega^2 \frac{R_s R_{ct} C_a C_d}{(R_{ct}C_a + R_s C_a + R_s C_d)} + \frac{1}{(R_{ct}C_a + R_s C_a + R_s C_d)} \quad (5)$$

A plot of $-\omega$ cot θ versus $-\omega^2$ is linear (not shown), and the ratio of the slope to the y-intercept is equal to $R_sR_{ct}C_aC_{dl}$. R_s and C_{dl} are measured independently by impedance spectroscopy and linear-sweep voltammetry, as described above, which allows the rate constant, k_s, to be determined from eq 4.

Alternatively, the ER response of the film is proportional to the admittance through the Faradaic portion of the equivalent circuit, and can be simulated by

$$\mathrm{Re}(\mathscr{R}_{ac}) \propto \frac{-C_a(1 - \omega^2 R_s R_{ct} C_a C_{dl})}{\xi} \quad (6a)$$

$$\mathrm{Im}(\mathscr{R}_{ac}) \propto \frac{C_a \omega (R_{ct}C_a + R_s C_a + R_s C_{dl})}{\xi} \quad (6b)$$

$$\xi = (1 - \omega^2 R_s R_{ct} C_a C_{dl})^2 + \omega^2 (R_{ct}C_a + R_s C_a + R_s C_{dl})^2 \quad (6c)$$

According to eq 6, the vertical line in Figure 7 at Re($\mathscr{R}_{ac}$) = 0 corresponds to the point at which angular frequency of E_{ac} is $\omega = (2k_s/R_sC_{dl})^{1/2}$.[24] By using the values of R_sC_{dl} for the amount of polymer deposited in each film obtained from Figure 3, k_s may then be determined.

Determinations of k_s as a function of the mole fraction of EDOT in the polymer using the methodologies described for eqs 5 and 6 are plotted in Figure 8. Both methods for determining k_s produced equivalent results. A linear (R^2 = 0.962) increase in apparent k_s occurred with increasing proportions of EDOT, ranging from $(3.1 \pm 0.3) \times 10^3$ s^{-1} for PEDTM to $(11.0 \pm 0.8) \times 10^3$ s^{-1} for PEDOT, independent of film thickness. The use of E_{ac} amplitudes ranging from 10 to 50 mV RMS did not significantly affect k_s, validating the linear approximation inherent in eqs 3 and 4. This result quantitatively demonstrates that the presence of the methanol substituent on EDTM significantly decreases the apparent switching rate of the polymer on ITO.

Niki and Sagara[24] showed that the maximum measurable k_s is inversely proportional to the RC time constant of the electrochemical cell and the detection limit of the ER response. In their studies of adsorbed hemin on glassy carbon the maximum measurable k_s was approximately 8×10^4 s^{-1} for a

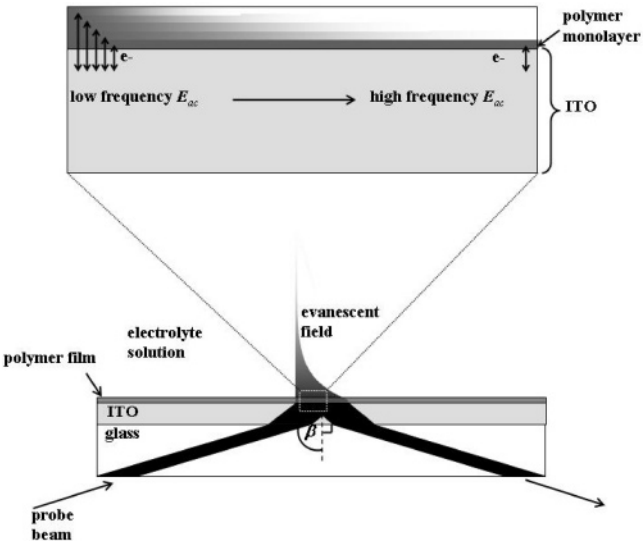

Figure 9. Schematic representation illustrating the surface selectivity of the ER response. At low frequency E_{ac} (left) the ER response is observed over several monolayers, indicated by the shaded polymer layers. As the frequency of E_{ac} is increased (right) the ER response is increasingly selective toward the fastest electrochromic processes, i.e., the first adsorbed monolayer.

cell time constant of 0.6 ms. In the ATR work presented here, a slightly smaller RC time constant (0.4 ms) and a similar detection method predict a comparable or slightly higher maximum measurable k_s. Thus if the measurable k_s was limited by the ATR spectroelectrochemical cell, the ER response would have reached a plateau at higher values of k_s. The linearity of the results plotted in Figure 8 shows that the apparent rates obtained for PEDOT/PEDTM polymer films were not limited by the kinetic constraints of the electrochemical cell.

Reynolds and co-workers[5,6] measured optical switching time in relatively thick (150−300 nm) films composed of PEDOT and PEDOT derivatives on ITO electrodes. Upon application of a potential step, the time required to obtain 95% of the full optical contrast ranged from 2 s for PEDOT to 0.3 s for poly-(dimethyl-3,4-propylenedioxythiophene).[5,6] They observed a decrease in switching time with increasing degree of substitution, or size, of the alkylenedioxy bridge of the monomer unit. This was attributed to differences in film density; the more highly substituted polymer being deposited in an expanded geometry offers less hindrance to counterion transport.[7]

Before comparing our results to those of Reynolds et al., it is important to note two important differences in the film properties and measurement techniques: (1) The films examined herein were 10−20 times thinner than those studied by Reynolds et al., and only about 1% of the full optical contrast of these films was achieved by application of an E_{ac} amplitude of 50 mV RMS.[5−7,9] This would certainly result in the measurement of a faster switching rate, but is not enough to account for the observed difference of 3 orders of magnitude in apparent rate. (2) The switching rates reported by Reynolds et al. were obtained by recording the thin film transmittance as a function of time in a single-pass transmission geometry, which is most representative of the bulk film.

In contrast, the ER response measures only optical changes in the film in response to the modulation of E_{ac} about E_{dc} and is therefore primarily selective toward the *fastest* electrochromic processes within the film, especially at high modulation frequencies. This hypothesis is illustrated in Figure 9. While the evanescent field effectively probes the entire thickness of the film (penetration depth ∼200 nm), the application of a high-frequency modulated potential selectively detects only those processes that are fast enough to occur on the time scale of the potential modulation. Since the electrochromism of the polymer is initiated by charge injection from the ITO substrate, the electrochromic process is initiated in the first adsorbed monolayer of polymer. Therefore, at high modulation frequencies, the ER response is likely to be most representative of redox-initiated changes in optical properties at the polymer/ITO interface, and the measured electrochromic switching rate, k_s, represents the high-speed limit for charge injection into the first adsorbed monolayer of the conducting polymer. This hypothesis is reinforced by an observed invariability in the ER response as a function of film thickness between 2 and 6 equivalent monolayers.

The results in Figure 8 contradict Reynolds' observation of slower switching rate with increasing substitution on the ethylenedioxy bridge. Given the near-surface selectivity of the ER response, the lower observed switching rate for PEDTM is likely due to the nature of the substituent, and its interactions with the ITO surface, rather than the physical structure of the bulk film. It is reasonable that the hydroxyl group of EDTM may hydrogen bond with terminal lattice In_2O_3 or oxy-hydroxide groups at the ITO surface,[62] hindering conformational changes along the polymer backbone associated with the electrochromic effect.

Conclusions

We have shown the first reported use of ER spectroscopy in a multiple reflection ATR geometry at an optically transparent electrode. The inherent frequency-dependent nature of the ER response permits selective analysis of fast electrochromic processes, even in the presence of slower electrochemical processes. For adsorbed films on electrode surfaces, this usually corresponds to analysis of the first adsorbed monolayer, even in a multilayer film. This technique was used to investigate the high-speed limit of electrochromic switching in PEDOT and PEDTM polymer and copolymer films.

The electropolymerization of thin films of PEDOT or PEDTM onto an ITO electrode resulted in a linear increase in capacitance as a function of the charge passed during polymerization, with identical results obtained for both polymers, indicating an approximately equal number of charge carriers within films composed of either polymer. Application of E_{ac} about the E_{mid} for the polymer redox reaction induces a sinusoidal change in the optical properties of the polymer film, which can be measured as a change in the reflectivity ($\mathscr{R}_{ac}$) at the ITO/polymer interface.

The ER response of the polymer films depends on the frequency of the potential modulation; it is constant at low frequencies and declines rapidly with increasing frequency. The cutoff frequency is significantly lower for PEDTM relative to PEDOT, indicating a slower switching rate for PEDTM. Quantitative determination of electrochromic switching rate, derived from the complex plane analysis of the ER response, shows a linear decrease from $11 \times 10^3\ s^{-1}$ to $3 \times 10^3\ s^{-1}$ with increasing proportions of EDTM monomer, suggesting that the electrochromic switching rate is limited by interactions of the hydroxyl substituent with the ITO surface. This effect could have significant implications for studies which seek to optimize the electron-transfer processes at ITO, and related electrodes, via surface modification with PEDOT-related polymeric systems, such as the current investigations utilizing a carboxylic acid derivatized PEDTM.[22]

Acknowledgment. S.S.S. and N.R.A. gratefully acknowledge support of this research from Grant No. DE-FG03-02ER15378 from Chemical Sciences, Geosciences and Biosciences Division, Office of Basic Energy Research, U.S. Department of Energy, and from the National Science Foundation (S.S.S., NSF CHE-0108805 and CHE-0518702; N.R.A., NSF CHE-0211900), and the NSF-Science and Technology Center−Materials and Devices for Information Technology (DMR-0120967). W.J.D. gratefully acknowledges partial support of this research by a fellowship from the Proposition 301 Initiative on Photonics, Arizona Board of regents.

References and Notes

(1) Doherty, W. J.; Armstrong, N. R.; Saavedra, S. S. *Macromolecules.* Submitted for publication.
(2) Groenendaal, L.; Zotti, G.; Aubert, P. H.; Waybright, S. M.; Reynolds, J. R. *Adv. Mater.* **2003**, *15*, 855.
(3) Krishnamoorthy, K.; Ambade, A. V.; Kanungo, M.; Contractor, A. Q.; Kumar, A. *J. Mater. Chem.* **2001**, *11*, 2909.
(4) Krishnamoorthy, K.; Kanungo, M.; Ambade, A. V.; Contractor, A. Q.; Kumar, A. *Synth. Met.* **2001**, *125*, 441.
(5) Kumar, A.; Welsh, D. M.; Morvant, M. C.; Piroux, F.; Abboud, K. A.; Reynolds, J. R. *Chem. Mater.* **1998**, *10*, 896.
(6) Welsh, D. M.; Kumar, A.; Meijer, E. W.; Reynolds, J. R. *Adv. Mater.* **1999**, *11*, 1379.
(7) Welsh, D. M.; Kumar, A.; Morvant, M. C.; Reynolds, J. R. *Synth. Met.* **1999**, *102*, 967.
(8) Gaupp, C. L.; Welsh, D. M.; Reynolds, J. R. *Macromol. Rapid Commun.* **2002**, *23*, 885.
(9) Gaupp, C. L.; Welsh, D. M.; Rauh, R. D.; Reynolds, J. R. *Chem. Mater.* **2002**, *14*, 3964.
(10) Sonmez, G.; Schwendeman, I.; Schottland, P.; Zong, K. W.; Reynolds, J. R. *Macromolecules* **2003**, *36*, 639.
(11) Schwendeman, I.; Gaupp, C. L.; Hancock, J. M.; Groenendaal, L.; Reynolds, J. R. *Adv. Funct. Mater.* **2003**, *13*, 541.
(12) Schottland, P.; Zong, K.; Gaupp, C. L.; Thompson, B. C.; Thomas, C. A.; Giurgiu, I.; Hickman, R.; Abboud, K. A.; Reynolds, J. R. *Macromolecules* **2000**, *33*, 7051.
(13) Sankaran, B.; Reynolds, J. R. *Macromolecules* **1997**, *30*, 2582.
(14) Krishnamoorthy, K.; Kanungo, M.; Contractor, A. Q.; Kumar, A. *Synth. Met.* **2001**, *124*, 471.
(15) Irvin, J. A.; Schwendeman, I.; Lee, Y.; Abboud, K. A.; Reynolds, J. R. *J. Polym. Sci., Part A: Poly. Chem.* **2001**, *39*, 2164.
(16) Havinga, N. N.; Mutsaers, C. M. J.; Jenneskens, L. W. *Chem. Mater.* **1996**, *8*, 769.
(17) Thompson, B. C.; Schottland, P.; Sonmez, G.; Reynolds, J. R. *Synth. Met.* **2001**, *119*, 333.
(18) Doherty, W. J.; Armstrong, N. R.; Saavedra, S. S. *Chem. Mater.* **2005**, *17*, 3652.
(19) Baba, A.; Lubben, J.; Tamada, K.; Knoll, W. *Langmuir* **2003**, *19*, 9058.
(20) Baba, A.; Knoll, W. *J. Phys. Chem. B* **2003**, *107*, 7733.
(21) Xia, C. J.; Advincula, R. C.; Baba, A.; Knoll, W. *Langmuir* **2002**, *18*, 3555.
(22) Marrikar, S.; Carter, C.; Evans, D.; Wysocki, R. J.; Armstrong, N. R. Manuscript in preparation.
(23) Feng, Z. Q.; Imabayashi, S.; Kakiuchi, T.; Niki, K. *J. Electroanal. Chem.* **1996**, *408*, 15.
(24) Feng, Z. Q.; Sagara, T.; Niki, K. *Anal. Chem.* **1995**, *67*, 3564.
(25) Sagara, T.; Igarashi, S.; Sato, H.; Niki, K. *Langmuir* **1991**, *7*, 1005.
(26) Sagara, T.; Murase, H.; Komatsu, M.; Nakashima, N. *Appl. Spectrosc.* **2000**, *54*, 316.
(27) Sagara, T.; Fukuda, M.; Nakashima, N. *J. Phys. Chem. B* **1998**, *102*, 2835.
(28) Sagara, T.; Fukuda, M.; Nakashima, N. *J. Phys. Chem. B* **1998**, *102*, 521.
(29) Sagara, T.; Niki, K. *Langmuir* **1993**, *9*, 831.
(30) Sagara, T.; Iizuka, J.; Niki, K. *Langmuir* **1992**, *8*, 1018.
(31) Brevnov, D. A.; Finklea, H. O. *J. Electrochem. Soc.* **2000**, *147*, 3461.
(32) Yamada, T.; Nango, M.; Ohtsuka, T. *J. Electroanal. Chem.* **2002**, *528*, 93.
(33) Yamada, T.; Hashimoto, T.; Kikushima, S.; Ohtsuka, T.; Nango, M. *Langmuir* **2001**, *17*, 4634.
(34) Riley, D. J.; Tull, E. J. *J. Electroanal. Chem.* **2001**, *504*, 45.
(35) Sagara, T.; Kato, N.; Kakashima, N. *J. Phys. Chem. B* **2002**, *106*, 1205.
(36) Toyota, A.; Nakashima, N.; Sagara, T. *J. Electroanal. Chem.* **2004**, *565*, 335.
(37) Gaigalas, A. K.; Niaura, G. *J. Colloid Interface Sci.* **1997**, *193*, 60.
(38) Gaigalas, A. K.; Reipa, V.; Vilker, V. L. *J. Colloid Interface Sci.* **1997**, *186*, 339.
(39) Feng, Z. Q.; Imabayashi, S.; Kakiuchi, T.; Niki, K. *J. Electroanal. Chem.* **1995**, *394*, 149.
(40) Feng, Z. Q.; Imabayashi, S.; Kakiuchi, T.; Niki, K. *J. Chem. Soc., Faraday Trans.* **1997**, *93*, 1367.
(41) Sagara, T.; Niwa, K.; Sone, A.; Hinnen, C.; Niki, K. *Langmuir* **1990**, *6*, 254.
(42) Ruzgas, T.; Wong, L.; Gaigalas, A. K.; Vilker, V. L. *Langmuir* **1998**, *14*, 7298.
(43) Avila, A.; Gregory, B. W.; Niki, K.; Cotton, T. M. *J. Phys. Chem. B* **2000**, *104*, 2759.
(44) Amemiya, T.; Hashimoto, K.; Fujishima, A. *J. Phys. Chem.* **1993**, *97*, 9736.
(45) Amemiya, T.; Hashimoto, K.; Fujishima, A. *J. Phys. Chem.* **1993**, *97*, 4187.
(46) Amemiya, T.; Hashimoto, K.; Fujishima, A. *J. Phys. Chem.* **1993**, *97*, 7, 4192.
(47) Amemiya, T.; Hashimoto, K.; Fujishima, A. *J. Electroanal. Chem.* **1994**, *377*, 143.
(48) Garcia-Canadas, J.; Meacham, A. P.; Peter, L. M.; Ward, M. D. *Electrochem. Commun.* **2003**, *5*, 416.
(49) Kim, S.; Wang, Z. H.; Scherson, D. A. *J. Phys. Chem. B* **1997**, *101*, 2735.
(50) Doherty, W. J.; Donley, C. L.; Armstrong, N. R.; Saavedra, S. S. *Appl. Spectrosc.* **2002**, *56*, 920.
(51) Lima, A.; Schottland, P.; Sadki, S.; Chevrot, C. *Synth. Met.* **1998**, *93*, 33.
(52) Akoudad, S.; Roncali, J. *Electrochem. Commun.* **2000**, *2*, 72.
(53) Bard, A. J.; Faulkner, L. R. *Electrochemical Methods*: *Fundamentals and Applications*, 2nd ed.; John Wiley & Sons: New York, 2001.
(54) Ge, C.; Doherty, W. J.; Mendes, S. B.; Armstrong, N. R.; Saavedra, S. S. *Talanta* **2005**, *65*, 1126.
(55) Dunphy, D. R. Dissertation, University of Arizona, 1998.
(56) Randriamahazaka, H.; Noel, V.; Chevrot, C. *J. Electroanal. Chem.* **1999**, *472*, 103.
(57) Garciajareno, J. J.; Navarro, J. J.; Roig, A. F.; Scholl, H.; Vicente, F. *Electrochim. Acta* **1995**, *40*, 1113.
(58) Saliba, R.; Agricole, B.; Mingotaud, C.; Ravaine, S. *J. Phys. Chem. B* **1999**, *103*, 9712.
(59) Bobacka, J.; Lewenstam, A.; Ivaska, A. *J. Elecroanal. Chem.* **2000**, *489*, 17.
(60) Lelievre, D.; Plichon, V.; Laviron, E. *J. Electroanal. Chem.* **1980**, *112*, 137.
(61) Laviron, E. *J. Electroanal. Chem.* **1979**, *97*, 135.
(62) Donley, C.; Dunphy, D.; Paine, D.; Carter, C.; Nebesny, K.; Lee, P.; Alloway, D.; Armstrong, N. R. *Langmuir* **2002**, *18*, 450.